MIXED MATRIX MEMBRANES COMPRISING SILICA-(ZIF-8) CORE-SHELL SPHERES WITH ORDERED MESO-MICROPOROSITY FOR NATURAL- AND BIO-GAS UPGRADING

Sara Sorribas, Beatriz Zornoza, Carlos Téllez*, Joaquín Coronas

Chemical Engineering Department and Nanoscience Institute of Aragón. Universidad de Zaragoza, 50018 Zaragoza, Spain

* Corresponding author:

Dr. Carlos Téllez Ariso

Chemical Engineering Department and Nanoscience Institute of Aragón

Universidad de Zaragoza

Campus Río Ebro. C/ Mariano Esquillor s/n. 50018 Zaragoza. Spain

Phone: 34 976 761000, Ext. 5429. Fax: 34 976 761879

e-mail: ctellez@unizar.es

ABSTRACT

Mixed matrix membranes (MMMs) containing meso-microporous silica-(ZIF-8) spheres (MSS-Z8) were prepared using polysulfone (PSF) Udel® as polymeric matrix, with loadings varying between 0 and 32 wt.%. The interaction between the filler and the polymer was studied by scanning electron microscopy and focused ion beam techniques, observing a good dispersion of the filler and an intimate contact between the ZIF-8 crystals shell and the polymeric matrix. X-ray diffraction indicated that the polymeric matrix did not alter the structure of the filler, and suggested the penetration of PSF chains into the flexible pores of the ZIF-8 crystals of the shell. MSS-Z8 MMMs were tested for the separation of CO_2/CH_4 and H_2/CO_2 mixtures at different temperatures (35-150 ºC) and CO_2/CH_4 feed compositions. For all equimolar mixtures, the selectivity remained almost constant with the filler content while the permeability increased, the best performance being achieved for 32 wt.% MSS-Z8 MMMs with an increase of almost 400 % for H_2 and 300 % for CO_2 in comparison with pure PSF. This enhancement in permselectivity resulted in Robeson´s 2008 upper bound for H_2/CO_2 separation being reached when the temperature was increased up to 120 ºC.

Keywords: Mixed matrix membranes, Gas separation, Mesoporous silica sphere, ZIF-8, Silica-(ZIF-8) core-shell spheres, Polysulfone.

1. INTRODUCTION

Natural gas, a hydrocarbon gas mixture consisting primarily of methane with other higher hydrocarbons (i.e. ethane, propane, butane), is the primary energy resource in the world and global consumption is projected to double from 2003 to 2030 [1]. Nowadays, alternative energy resources such as biogas, a methane rich gas (55-60 %) [2] produced by the breakdown of organic matter (biomass) in the absence of oxygen, are attracting considerable attention. Both raw natural gas and biogas require purification treatment to reduce undesirable impurities such as hydrogen sulfide, nitrogen, water, and carbon dioxide before the gas can be used as fuel. The typical concentration of the most common pollutant, CO_2 , is between 5-25 mol%, which needs to be reduced to less than 2% to meet pipeline specifications due to its acidic and corrosive properties[3]. In addition, rising carbon dioxide emissions in the environment leads to global warming which constitutes an issue of exceptional concern today. On the other hand, hydrogen appears to be one of the most promising combustibles for a sustainable future. A method of hydrogen production is by fermentation using carbohydrate rich substrates, where carbon dioxide is also a product. Once again, the CO_2 must be eliminated to enrich and purify H_2 from the gaseous mixture for any application (e.g. in fuel cells)[4].

One way to reduce CO_2 emissions is to capture it from power plants. Various techniques have been proposed for this purpose including chemical absorption, physical absorption, pressure swing absorption, temperature swing absorption, cryogenic distillation and separation via membranes [5, 6]. In the 1980s, absorption techniques were reported to be the only competitive methods for flue gas treatment [7].

Membrane technology generally provides several advantages over the above-mentioned conventional separation techniques including low capital cost and ease of processing. This technology is relatively easy to operate and control. In particular,

membranes constitute a low cost way of separating gases when high purity gas streams are not needed. Polymer membranes, for instance UOP Separex™ cellulose acetate membranes, have already been successfully used for natural gas upgrading [8].

However, there appears to be a trade-off between permeability and selectivity for polymer membranes, where a highly selective membrane tends to have low permeability and *vice versa*. This inverse permeability/selectivity behavior was illustrated by Robeson in 1991 [9], updated in 2008 [10]. In recent years, different strategies such as the synthesis of new polymers with improved performance, the modification of the properties of existing polymers, the combination of two polymers in a membrane (copolymer membranes), or the fabrication of mixed matrix membranes (MMMs) have been proposed [11]. In the latter strategy, the use of two materials with different gas separation behaviors offers the possibility of designing an efficient membrane, allowing the combination of the advantages of both phases: easy processability and low cost of the polymer with the superior gas separation performance of the nanostructured fillers [12]. Also, the incorporation of these specific "ingredients" within the polymeric matrix generally provides enhanced physical, mechanical and thermal properties for use in aggressive environments and provides a membrane stabilization system against change in permeability with the temperature [13].

The integration of zeolites into polymeric membranes has attracted much attention, but the zeolite and polymer often have a poor interaction, producing non-selective void spaces between the zeolite particles and the polymeric matrix which leads to a decrease in selectivity [12, 14, 15]. ~~In addition, mesoporous MCM-41 spheres~~ On the other hand, spherical particles of ordered mesoporous silica with high mechanic and thermal stability, facility of chemical functionalization, high specific surface areas (>500 m^2/g), and well defined bimodal pore size distribution (2.7 nm pores, typical of MCM-41

hexagonal array, and larger mesopores of 15 nm) have been incorporated as filler to enhance the inorganic filler/polymer interaction and to increase the permeability due to their mesoporosity. Using these materials, and taking into account that the cross sectional areas per chain of the most synthetic polymers are around 1 nm^2 or less, these polymer chains can penetrate through the mesoporosity, ~~thus blocking~~ enhancing the contact [14]. However, this fact could block the large pores of the silica and make ~~making~~ the inner ones almost inaccessible [15].

Metal-organic frameworks (MOFs) have appeared as a new class of crystalline and porous materials built from metal ions as connectors and organic bridging ligands as linkers[16]. MOF-MMMs are promising next-generation membranes for gas separation [17, 18]. Compared to traditional fillers, the interaction of both phases is easier to control due to the better affinity of the MOF linkers with the polymer chains. Furthermore, the size, shape, and chemical functionalities of the MOF cavities can be easily adjusted by choosing the appropriate linker-metal couples [19].

Among MOFs, ZIF-8 (Zn(2-methylimidazole)$_2$) in particular has been one of the most extensively studied prototypical ZIF (Zeolitic imidazolate framework) porous solids, with large pores of 11.6 Å connected through small apertures of 3.4 Å, outstanding high thermal stability (up to 400ºC) and of a hydrophobic character [20]. In addition, its flexible nature enables the adsorption of molecules larger than 3.4 Å. ZIF-8 was first used as a filler embedded in PDMS (polydimethylsiloxane) membranes for solvent resistant nanofiltration (SRNF) [21]. Concerning gas separation, ZIF-8 based MMMs have frequently been prepared with the polyimide Matrimid® for CO_2/CH_4, CH_4/N_2, CO_2/C_3H_8 and H_2/C_3H_8 separations with loadings up to 80 wt.% [22]., In the form of asymmetric membranes, ~~for~~ the separation of CO_2/CH_4 and CO_2/N_2 binary gas mixtures ~~in the form of asymmetric membranes~~has been studied [2]. In addition, the

influence of different sonication powers before membrane casting in~~, for~~ CO_2/CH_4 separation ~~employing different sonication powers before membrane casting~~ [23], and ~~using~~ the use of ZIF-8 nanoparticles (around 60 nm in size) for H_2, CO_2, O_2, N_2 and CH_4 pure gas permeation [24] have been reported. ZIF-8 has also been added to Ultem® polymer matrix to prepare mixed matrix dual-layer hollow-fiber composite asymmetric membranes for CO_2/N_2 separation [25]. ZIF-8 has also been incorporated into 6FDA-based polyimides to form MMMs for C_3H_6/C_3H_8 [26, 27], CO_2/N_2 [28] or CO_2/CH_4 [27] separation processes and performing surface cross-linking for hydrogen purification [29]. This MOF material has also been added to PPEES (poly-(1, 4-phenylene ether-ether-sulfone)) for O_2/N_2, H_2/N_2, H_2/CH_4, CO_2/CH_4, and C_2H_4/C_2H_6 separations [30], embedded in PIM-1 (polymer of intrinsic microporosity) for H_2/N_2, He/N_2, O_2/N_2 and CO_2/CH_4 separations [31] or used alone and/or in combination with zeolites (silicalite-1) on PSF (polysulfone) for H_2/CH_4, O_2/N_2, CO_2/N_2 and CO_2/CH_4 mixed gas separations [32]. In PSF, ZIF-8 has contributed to gas permeation by increasing the gas solubility of CO_2 [33]. Finally, ZIF-8/ polybenzimidazole MMMs have recently been tested for H_2/CH_4 separation up to 230 ºC [34, 35].

Despite the wide variety of published studies on MMMs comprising ZIF-8 as filler, none of them has explored the use of this particular hydrophobic microporous MOF phase in combination with a hydrophilic mesoporous structure in the same particle. In this work, the recently described compound comprising silica-(ZIF-8) core-shell spheres with tunable ordered meso-microporosity (called MSS-Z8) [36] has been employed as filler in a PSF polymer matrix for the preparation of MMMs for CO_2/CH_4 and H_2/CO_2 gas separation. The use of this material facilitates the production of highly homogeneous MMMs, improving dispersion and interaction with the polymer due to the fact that micron size particles avoid agglomeration and the spherical shape helps to

reduce the surface contact between filler particles within the polymer [~~35~~37, ~~37~~38]. In addition, these capsules enhance the permselectivity properties of pure polysulfone, since MSS-Z8 MMM selectivity is directly related to the micropore size of the ZIF-8 crystallites, forming the capsule walls, and permeability is increased due to the mesoporosity of silica sphere cores.

2. EXPERIMENTAL SECTION

2.1. Materials

For the synthesis of silica spheres, cetyltrimethylammonium bromide (CTABr, >98%), sodium metasilicate (Na_2SiO_3), and ethylacetate ($CH_3COOC_2H_5$, 99.9%) were used. Zinc nitrate hexahydrate ($ZnNO_3{\cdot}6H_2O$, >98%), 2-methylimidazole ($C_4H_6N_2$, >99%,) and methanol (99.99%) were used for the synthesis of ZIF-8 shells. Polysulfone (PSF, M_W 35000) and chloroform >99% were used for the MMMs preparation. All this materials were purchased from Sigma-Aldrich.

2.2. MSS-Z8 synthesis

MSS-Z8 filler was prepared in accordance with the procedure described in the literature[36]. For the synthesis of mesoporous silica spheres (MSSs) of ~3 μm [~~38~~39], the molar composition used was $1.5Na_2SiO_3$:1CTABr:$361H_2O$:$7.4CH_3COOC_2H_5$. For this, 3.92 g CTABr and 2 g of Na_2SiO_3 were dissolved in 70 mL of water. Then, 8 mL of ethylacetate was added under stirring for 30 s. After that, the solution was kept in a closed polypropylene flask at room temperature for 5 h, and then maintained at 90 ºC for 50 h. The product obtained was filtered in distilled water and ethanol, and calcined at 600 ºC for 8 h to remove the surfactant and activate the mesoporous structure. To create the ZIF-8 shell around the MSSs, an “in-situ” seeding process was developed, mixing 0.2 g of MSSs with a gel with a molar ratio of Zn^{2+}:2-

methylimidazole:H_2O=1:70:1238. Details of the process have already been published for the synthesis of ZIF-8 nanocrystals [~~39~~40]. After the seeding process, two steps of crystal growth were carried out to create a continuous ZIF-8 shell around the MSSs. For each step, 0.47 g $Zn(NO_3)_2 \cdot 6H_2O$ was dissolved in 10 mL of MeOH and 10 mL of water. In addition, 1 g 2-methylimidazole was dissolved in 10 mL of MeOH and 0.14 g of "in situ" seeded MSSs was added. The two solutions were sonicated for 5 min and mixed under vigorous stirring, maintaining the agitation for 2 h at room temperature. The final product was then collected by centrifuging with DI water and MeOH several times, decanted in MeOH to separate the spheres from non-attached nano-sized ZIF-8 particles and dried overnight.

2.3. Membrane fabrication

MSS-Z8 MMMs were prepared as follows. Firstly, 3.6 g of chloroform and the amount of MSS-Z8 necessary to obtain the required loading (8-32 wt.%), always in a proportion of 90/10 wt.% solvent/(MSS-Z8 + polymer), were mixed for 30 min in an ultrasonic bath. Polysulfone was then added, and the mixture was stirred overnight. The solution was then sonicated with three intervals of 15 min to ensure a well dispersed solution, cast on a flat glass plate and then left overnight partially covered to slow down the natural evaporation of solvent under ambient conditions. Once dried, the films were placed for 24 h under 1 kPa pressure in a vacuum oven at 120 ^{o}C to remove the remaining solvent.

2.4. Membrane characterization

MMMs were characterized by scanning electron microscopy (SEM) using an Inspect F scanning electron microscope to evaluate the dispersion of the filler through the membrane and the contact between the MSS-Z8 and the polymeric phase. Cross

sections were prepared by freeze-fracturing after immersion in liquid N_2 and subsequently coated with 15 nm gold. To verify the good contact between the ZIF-8 shell and the polymer, SEM images using the focused ion beam (FIB) technique were taken while the membrane was cut by accelerating concentrated gallium ions to a specific site. To distinguish the Si of the silica core, the Zn of the ZIF-8 shell and the carbon of the polysulfone, EDX mapping was also carried out.

Differential scanning calorimetry (DSC) measurements were made using Mettler Toledo DSC822^e equipment to calculate the glass transition temperature (T_g) of the MMMs at different filler loadings. Small pieces of dried membranes were transferred to 40 μL aluminum pans and hermetically sealed with aluminum covers. The samples were scanned from room temperature to 250 ^oC with a heating rate of 20 ^oC/min in two consecutive runs. The reported T_g values were calculated from the middle point of the slope transition in the second run, taking the average of two samples.

Thermogravimetric analysis (TG) was performed simultaneously on Mettler Toledo TGA/DTA 1 Start system equipment. Samples (10 mg) placed in 70 μL alumina pans were heated in an air flow (96 cm^3(STP)/min) up to 700 °C at a heating rate of 10 ^oC/min for calculating the percentage of filler and the thermal stability of the MMMs.

CO_2 adsorption isotherms were measured with Micrometrics ASAP 2020 equipment at 35 °C using water as a coolant.

Both filler and MMMs with different MSS-Z8 content were characterized by X-ray diffraction (XRD) at room temperature on a D-Max Rigaku diffractometer with a copper anode and a graphite monochromator to select the Cu-$K_{\alpha 1}$ radiation (λ= 1.5418 Å).

Attenuated total internal reflection Fourier transform infrared (ATR-FTIR) spectroscopy of the MMMs was performed on a bruker Vertex 70 FTIR (Billerica, MA)

spectrometer equipped with a deuterated triglycine sulfate (DTGS) detector and a Golden Gate diamond ATR accessory. Spectra were recorded by averaging 40 scans in the 4000-600 cm^{-1} wavenumber range at a resolution of 4 cm^{-1}. The Fourier transformed infrared spectroscopy (FTIR) absorption spectra of the powder samples (MSSs, ZIF-8 crystals and MSS-Z8) were acquired at room temperature with an Iraffinity Shimadzu spectrophotometer. Spectra of the samples corresponded to 30 scans at a resolution of 4 cm^{-1}, using the KBr pellet technique.

2.5. Permeation measurements

For permeation tests, a 13.8 cm^2 membrane area was cut from the film and introduced into a module consisting of two stainless steel pieces and a 316LSS macroporous disk support with a 20 µm nominal pore size. The membrane was ~~gripped~~ sealed inside with Viton o-rings. The gas permeation equipment is described ~~elsewhere .~~ in Fig. 1. For equimolar mixtures, 25/25 cm^3(STP)/min CO_2/CH_4 or H_2/CO_2 stream was fed at 330 kPa to the retentate side of the membrane using flow-mass controllers, while the permeate side of the membrane was swept with a 2 cm^3(STP)/min mass-flow controller stream of He (for CO_2 mixtures) or Ar (for H_2 mixtures) at 125 kPa. Concentrations of CO_2, H_2 and CH_4 in the outgoing streams were analysed by an Agilent 3000A online gas microchromatograph equipped with a thermal conductivity detector. Permeability was calculated in Barrer ($1 \cdot 10^{-10}$ cm^3(STP)·cm/(cm^2·s·cmHg)) once the exit stream of the membrane was stabilized, and the separation selectivity was calculated as the ratio of permeabilities. The membrane module was placed in a UNE 200 oven (Memmert, Schwabach, Germany) to control the temperature of the experiments.

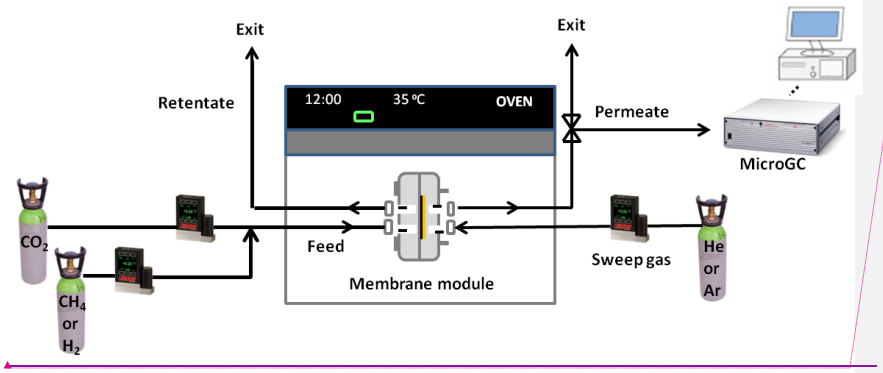

Fig. 1. Schematic of gas permeation equipment

The H_2, CO_2 and CH_4 permeabilities obtained at different temperatures in pure PSF, 16 and 32 wt.% MSS-Z8 MMMs were analyzed with the Arrhenius equation:

$$P = P_0 \exp\left(\frac{-E_p}{RT}\right) \qquad \text{Eq. 1}$$

where P is the permeability of the gas (Barrer), P_0 is the pre-exponential factor with the same units as the permeability, R is the universal gas constant (8.314 J/(mol·K)), T is the absolute temperature (K) and E_P is the apparent activation energy of permeability (kJ/mol).

3. RESULTS AND DISCUSSION

3.1. Characterization of MSS-Z8/PSF membranes

In our previous article [36], silica–(ZIF-8) core–shell spheres (MSS-Z8) were synthesized and characterized. The MSS-Z8 depicted an X-ray pattern similar to that of ZIF-8 crystals and the inner structure formed by the mesoporous silica core was confirmed by LA-XRD. Consistent with this, nitrogen adsorption-desorption measurements of the MSS-Z8 showed adsorption of N_2 due to both the micropores of the ZIF-8 shells and the bimodal pore distribution (pores around 2.7 and 10 nm) present

Con formato: Fuente: Times New Roman, 12 pto

in the mesoporous silica core spheres. The BET area of MSS-Z8 was 1005±45 m^2/g, with a total volume of 0.64 cm^3/g and a microporous volume of 0.31 cm^3/g.

TGA analyses (not shown) were carried out to calculate the real loading of MSS-Z8 in the membrane ~~(not shown)~~. For that, the percentage of remaining material after being heated to 700 ºC, ~~was~~ attributed to both the silica core and the ZnO obtained after the decomposition of the ZIF-8 shells, was used for calculations. TGA loading was in good agreement with the nominal values shown in Table 1. Regarding the glass transition temperature (T_g), in general the values of the MMMs were slightly higher than those of the unfilled PSF membrane but falling within experimental error (see Table 1). This suggests a good filler-polymer compatibility provided by the shell ZIF-8 crystals, since silica spheres without ZIF-8 coating showed rigidification of the polymer, with a Tg increase from 188.5ºC for pure PSF to 196 ºC for 16wt.% MSS MMM [~~35~~37]. It can be said that Tg was independent of the filler content, as occurred in previous works using ZIF-8 as filler in polysulfones [30]. Using other kinds of polymers, polyimide [3,28] or copolyimide [32], the Tg did not appear to change much with the loading of ZIF-8, but polybenzimidazole(PBI)/ZIF-8 MMMs [~~40~~41] had a much higher Tg than the bare polymer, suggesting a chain rigidification of this polymer.

Fig. 2~~1~~a-c shows SEM images of cross section views of MSS-Z8 MMMs with different loadings (8-32 wt.%). The filler is distributed homogeneously within the polymer and across all the thickness of the membrane (80 ± 10 µm), and no sedimentation is observed. In Fig. ~~1d~~2d, the MSS-Z8 core-shell structure is clearly observed with a homogeneous well-intergrown ZIF-8 shell with a thickness of approximately 500 nm. In addition, an intimate filler-polymer interaction is indicated by the SEM images, strong enough to break up the MSS-Z8 into two parts when the membrane is freeze-fractured after immersion in liquid N_2. The inorganic/organic

hybrid nature of the ZIF-8 shell as well as its hydrophobic character could be the reason for this strong interaction with the polymer Udel®.

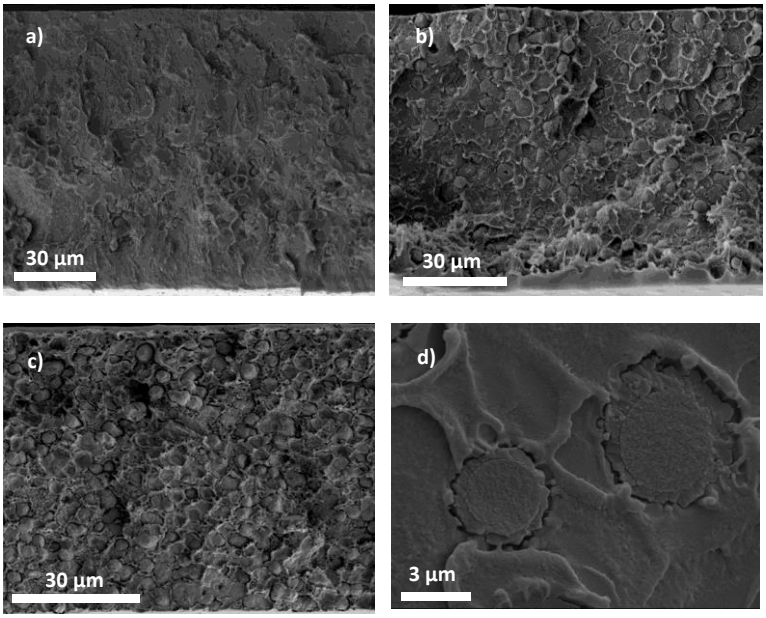

Fig. ~~1~~2. SEM images of cross-sections of MSS-Z8 MMMs: a) 8 wt.%, b) 12 wt.%, c) 32 wt.%, d) detail of panel b).

To prove that the interfacial gaps observed between the polymeric phase and the particulate phase were induced by the mechanical fracturing of the membranes, as occurred in previous works [22], the MMMs were also characterized by FIB (Fig. ~~2~~3). This technique allows cutting the membrane with high precision (up to 5 nm) obtaining a smooth surface, as previously done with MMMs comprising NH_2-MIL-53 and polyimide Matrimid® [~~41~~42]. In addition, unlike SEM, the gold covering did not affect the image, since it was removed in the first cuttings. Both secondary electron detector (SE) (Fig. ~~2.~~3a, b) and backscattered electrons (BSE) (Fig. ~~2c~~3c) were used to create the images. No interfacial gaps between the spheres and the polymeric phase were observed with either detector.

The EDX mapping (Fig. ~~2a~~3a, inset) shows that the Zn element coming from the ZIF-8 shells (green) and the Si element corresponding to the silica cores (blue) were homogeneously distributed in the polymeric matrix (red part corresponding to C atoms). The membranes were flexible up to 32 wt.% loading (Fig. ~~3~~4). Membranes with higher concentrations of filler were not analyzed, since they became brittle and cracked easily, as occurred in studies using ZIF-8 [24]. In fact, some studies [2] have shown that MOF-type filler loadings higher than 30 wt.% may deteriorate the properties of the MMMs.

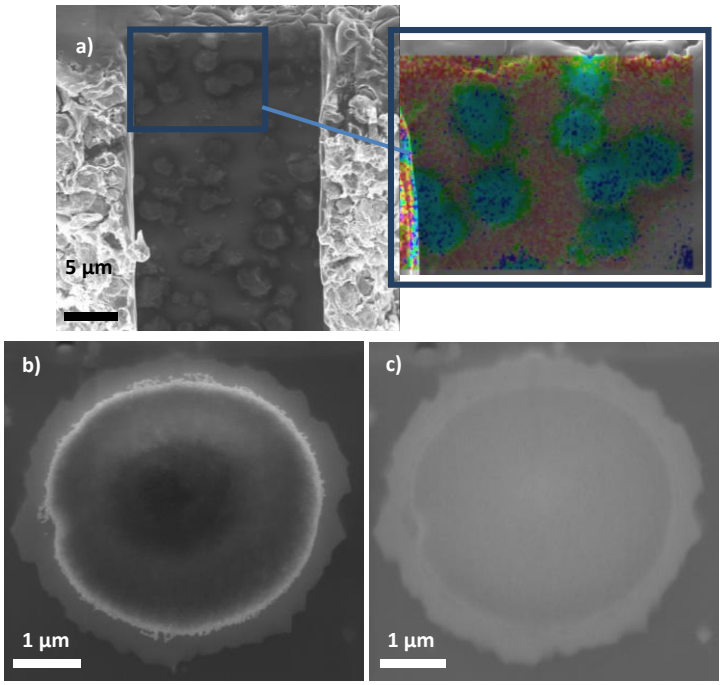

Fig. ~~2~~3. SEM images after FIB of cross-section 32 wt.% MMM: a) general image with an inset corresponding to EDX mapping (Zn green, Si blue and carbon red)), and individual silica@ZIF-8 sphere using b) SE and c) BSE detectors.

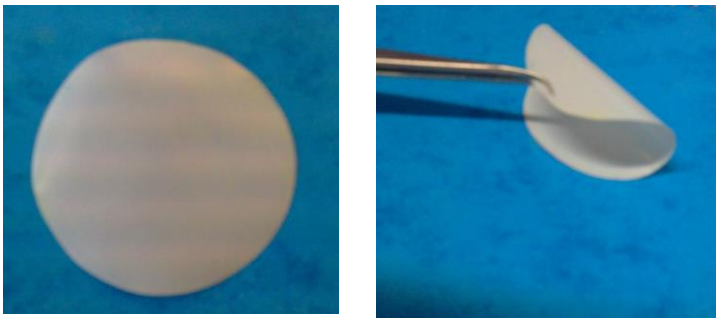

Fig. ~~3~~4. Images of 32 wt.% MMM treated at 120 ºC.

X-ray diffraction confirmed that the polymeric matrix did not alter the ZIF-8 structure of the filler (Fig. ~~4~~5), since the XRD pattern of the MMMs matches the pattern of the filler and the ZIF-8 signal increases with the filler loading. The first reflection at 7.4º is related to the ZIF-8 pore size and it has been shown that its intensity decreased when the pore was filled with other molecules, such as caffeine [~~42~~43]. The intensity ratio (r) of the first and the second peak area, at 7.4º and 10.4º respectively, were calculated for MSS-Z8 and for 32 wt.% MMM, being $r_{MSS\text{-}Z8}$=11.6 and r_{MMM}=5.3. This decrease in r when MSS-Z8 particles were embedded into the polymeric matrix can be explained by the penetration of PSF chains into the pores of the ZIF-8 crystals of the shell. ~~PSF shows an inter-chain spacing of 0.52 nm [14] while ZIF-8 contains large cavities of 1.16 nm which are accessible through small apertures of 0.34 nm.~~ Rather than static in nature, ZIF-8 exhibits a flexible framework structure [~~42~~43, ~~43~~44].

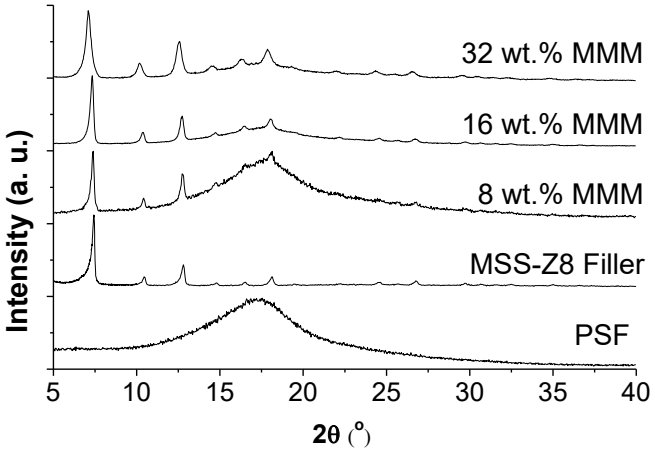

Fig. 45. XRD patterns of PSF, MSS-Z8 and MMMs (8-32 wt.% loading).

The ATR-FTIR spectra of bare PSF, MSS-Z8 filler and 32 wt.% MMM in the 1700-700 cm^{-1} wavenumber range are shown in Fig. 56. The 32 wt.% MMM sample was chosen to highlight the possible effect of the filler-polymer interaction. The spectrum of MSS-Z8 correlates well with the data of ZIF-8 crystals given in the literature [20, 24], where the C-N adsorption bonds are found in the 1100-1400 cm^{-1} range. In addition, in this sample there are broad adsorption peaks characteristic of MSSs at around 1230, 1070 and 800 cm^{-1}, characteristic of asymmetric (longitudinal optical (LO) and transversal optical (TO) modes) and symmetric Si-O-Si stretching vibration, respectively [35]. The PSF membrane spectrum shows several peaks between 900-800 cm^{-1} assigned to C-H rocking. The peaks in the 1100-1000 cm^{-1} region are assigned to C-C stretching, the peaks at 1147 cm^{-1} and 1324 cm^{-1} to Ar-SO_2-Ar symmetric stretching and the peak at 1235cm^{-1} to Ar-O-Ar stretching vibration [3537]. The 32 wt.% MSS-Z8 MMM spectrum shows the adsorption peaks assigned to MSS-Z8 and pure PSF, with a slight shift to higher wavenumbers (3 cm^{-1}) in the PSF peak assigned to Ar-O-Ar stretching vibration at 1235cm^{-1}. The shift could be due to the hydrogen

atoms of the double carbon bond of 2-methylimidazole in the ZIF-8 shell which could interact via hydrogen-bonding with the aryl ether groups of the polymer [~~35~~37, ~~42~~43], although it is in the same order as the resolution of the FTIR equipment.

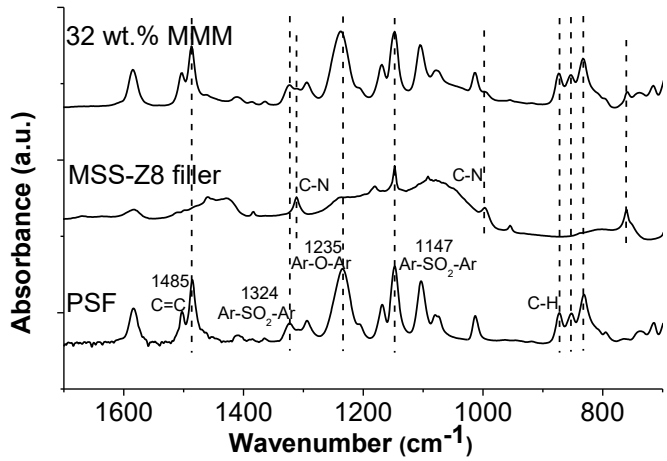

Fig. ~~5~~6. FTIR spectra of PSF, MSS-Z8, and 32 wt. % MSS-Z8 MMM.

3.2.Gas separation measurements

Permeability measurements for CO_2/CH_4 at different temperatures (35, 60, 90, 120 and 150 ^oC) and at different MSS-Z8 loadings up to 32 wt.% were carried out. The MMM of 32 wt.% loading was also tested for a H_2/CO_2 equimolar mixture at different temperatures. For 16 wt.% MSS-Z8 MMM, gas mixtures of CO_2/CH_4 at different feed compositions (50:50 mol%, 10:90 mol%, 90:10 mol% and single gas) were also tested.

It is worthy to mention that at loadings higher than 32 wt.% the membranes broke during the permeation experiments, probably due to the particles agglomeration phenomenon and low amount of polymer surrounding the spheres.

3.2.1. Influence of loading

Fig. ~~6~~ 7 shows CO_2 permeability and CO_2/CH_4 selectivity of MSS-Z8 MMMs with different filler loadings, from 0 to 32 wt.%. The measurements were performed with equimolar CO_2/CH_4 mixtures at 35 ºC and, to assess reproducibility, each percentage of loading was tested for three different membranes. The error of the measurements was calculated as the standard deviation percentage [(standard deviation/average) x 100]. All the results for MMMs exhibited a precision higher than 10 %.

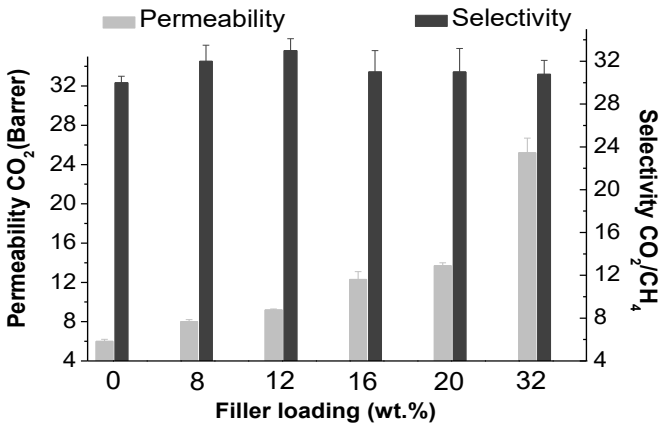

Fig. ~~6~~7. Gas separation results for MSS-Z8 MMMs at different loadings (0-32 wt.%) for equimolar CO_2/CH_4 mixtures at 35 ºC. Error bar corresponds to standard deviations.

The CO_2 adsorption capacity of the filler at 35 ºC and 1 atm (1.91 mmol/g, measured in the laboratory) is much higher than that of pure PSF (0.22 mmol/g [~~44~~45]). In addition to an enhancement in CO_2 adsorption when the filler is incorporated, the mesoporous phase of the silica core with bimodal pore distribution (2.7 and 10 nm) may favor gas diffusivity. Also, it cannot be ruled out, as indicated by other authors [33], that ZIF-8 increases the distance between polymer chains creating more polymer free volume [22]. As expected, CO_2 permeability increased with filler loading, leading to an

increment of 300 % in comparison with bare PSF when 32 wt.% MSS-Z8 were added, from 6.1±0.2 to 24.4±1.5 Barrer. CO_2/CH_4 selectivity gave a maximum of 33±1.1 at 12 wt.% MMM, although it remained almost constant for the different filler percentages, being 31±0.6 for the bare polymer. The fact that there was no loss of selectivity at high MSS-Z8 loadings was due to the good contact between the filler and polymer, as observed by the SEM images (Fig. ~~1~~2, Fig. 3), which avoided the generation of small non-selective voids. On the other hand, the 3.4 Å pore of the ZIF-8 shell covering the mesopores of the silica core should have promoted the transport of CO_2 (3.3 Å) over CH_4 (3.8 Å) due to the molecular sieving effect. However, in agreement with the literature [2, 26, 27], the addition of ZIF-8 markedly increased the permeability but not the selectivity for CO_2/CH_4 separation.

Comparing the result obtained for 16 wt.% MSS-Z8 MMMs with that reported in the literature for 16 wt.% ZIF-8 MMM [32], an enhancement in selectivity from 19.8 using ZIF-8 crystals to 31.8 using MSS-Z8 as filler was observed, while the permeability remained almost constant (12.3 and 12.1 Barrer for MSS-Z8 and ZIF-8, respectively). The improvement in selectivity could be attributed to a better contact established between the polymer and the external roughness of the MSS-Z8, composed of hundreds of crystals creating an interpenetrated network. This behavior has been observed previously in the literature [~~37~~38], where hollow silicalite-1 spheres used as filler had better contact with the polymer matrix than bare silicalite-1 crystals. In addition, the use of small crystals may favor their aggregation, forming a grape-like morphology with non-selective holes between the particles [23, 24]. Comparing with other PSF-based membranes reported, i. e., 16 wt.% HKUST MMM and 16 wt.% silicalite-1 MMM [32], both CO_2 permeability (8.8 and 9.6 Barrer respectively) and CO_2/CH_4 selectivity (15.7 and 12.07 respectively) are lower than those values obtained

with 16 wt.% MSS-Z8 MMM. These comparisons highlight the promising results obtained by using this new filler, which could be able to exceed the Robeson upper limit embedded in other polymeric matrix with better performance than PSF by itself. For example, by using the polymer 6FDA-DAM, which is close to the upper bound 1991, the MSS-Z8 could be able to reach the upper bound 2008, as occurs when ZIF-90 is added [46].

3.2.2. Influence of temperature

A high temperature operation in industrial applications would allow: i) a better performance (as will be shown), and ii) energy cost savings in terms of reduction in gases temperature from process prior the separation [~~45~~47]. To study the stability of the membrane and the influence of the temperature on the permselectivity properties, experiments at different temperatures (35-150 ºC) with equimolar CO_2/CH_4 and H_2/CO_2 mixtures were carried out. ~~Fig. 7 illustrates the effect of varying the temperature on the selectivity versus permeability for 32 wt.% MSS-Z8 MMMs and bare polymer.~~ The E_p of all the gases for pure PSF membrane, and 16 and 32 wt.% MMMs, are given in Table 2, calculated from their respective equimolar mixtures, with R^2>0.99 in all gases (Fig. 8).

Comentado [U1]: Ref. 2, comment 11

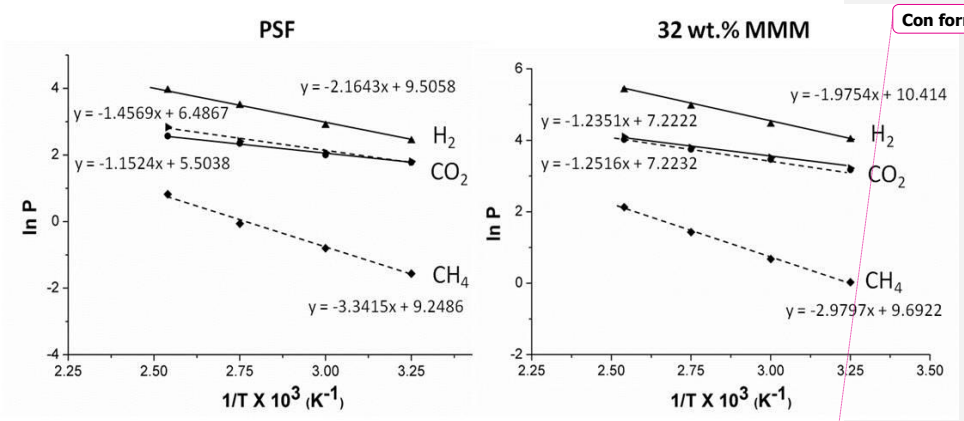

Fig. 8. The Arrhenius plots of PSF and 32 wt.% MMM. Continuous lines: H_2/CO_2 mixture; dotted lines: CO_2/CH_4 mixture.

Fig. ~~7~~9 illustrates the effect of varying the temperature on the selectivity versus permeability for 32 wt.% MSS-Z8 MMMs and bare polymer. For all the mixtures and membranes, both CO_2 and H_2 permeabilities showed a typical activated diffusion behavior and at all the temperatures the 32 wt.% MMM performed better than pure polymer, showing much higher permeabilities with similar selectivities ~~(Fig. 7)~~.

In the CO_2/CH_4 mixture for 32 wt.% MSS-Z8 MMMs, an increase of nearly 200 % for CO_2 (from 24.4 Barrer at 35 ºC to 73.1 Barrer at 150 ºC) was observed. For this membrane, H_2 permeability increased almost 300 % for the H_2/CO_2 mixture (from 56.1 to 224.1 Barrer) when the temperature was increased from 35 to 120 ºC. This enhancement in permeability with temperature was due to an increase in diffusivity of the gas as well as an enhancement in flexibility of the polymer chains. The pronounced decrease in selectivity for the CO_2/CH_4 mixture is a combination of the increase of the free volume of the membrane and a favored diffusion of CH_4 versus CO_2 with the temperature (in fact, $E_P(CH_4) > E_P(CO_2)$). Nevertheless, for the H_2/CO_2 mixture the selectivity increased with the temperature, since $E_P(H_2) > E_P(CO_2)$. It should be considered that the gas transport through the membranes entails solution and diffusion;

accordingly, in both mixtures the selectivity trends could be explained in relation with the CO_2 solubility declining with temperature. A similar behavior with the temperature has been observed for 30 wt.% /ZIF-8/PBI [34]. Notice for 32 wt.% MSS-Z8 MMMs that when the temperature was cooled down again to 35 ºC, the CO_2/CH_4 selectivity remained constant at 31 but the permeability increased from 24.4 to 28.9 Barrer. This effect may be due to desorption at high temperatures of some impurities present in the pores of MSS-Z8.

With the permselectivity enhancement for H_2/CO_2 separation achieved with the incorporation of 32 wt.% MSS-Z8, the upper-bound line estimated by Robeson in 2008 [10] pointing towards a commercially attractive region was reached when increasing the temperature until 120 ºC (Fig. ~~7~~9). However, the permeability-selectivity values for CO_2/CH_4 are located below 2008 Robeson´s upper bound when increasing the temperature.

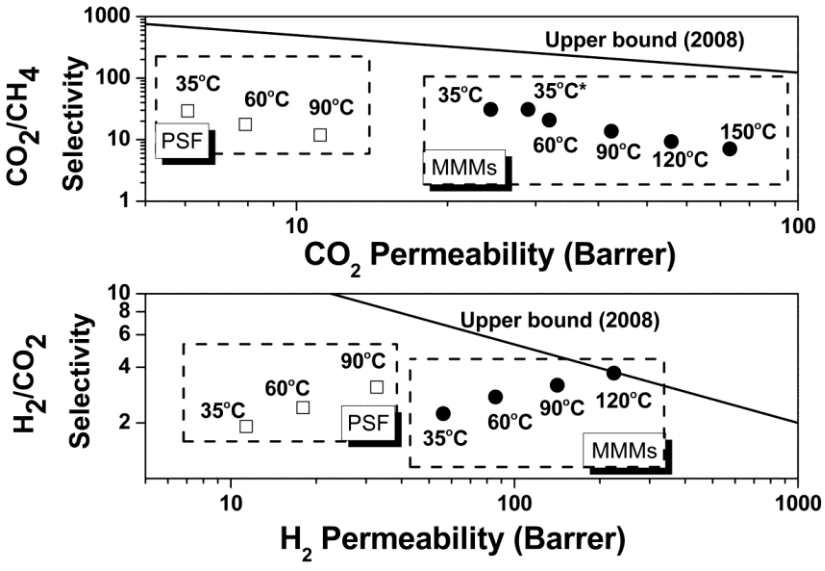

Fig. ~~7~~9. Results of 32 wt.% MMM (closed symbols) and PSF (open symbols) at different temperatures for CO_2/CH_4 and H_2/CO_2. For CO_2/CH_4 mixture, 35 ºC* corresponds to the measure obtained after the temperature was cooled down again to 35 ºC.

3.2.3. Influence of gas composition

The permeation of gases in a mixture may differ from that of a single gas because of the competition among permeating gases for the sorption sites of the membrane and between the mobility of gases through the membrane [~~46~~48]. In addition, if CO_2 permeates through the membrane, the plasticization effect influences the transport through membranes. Because of all these features, and taking into account that the compositions of biogas and natural gas are not constant, the performance of MMMs for CO_2/CH_4 separation for different gas compositions was studied. Fig. ~~8~~ 10 shows the influence of the CO_2 feed partial pressure on the selectivity and the CO_2 flow (cm^3 STP/min) for pure PSF and 16 wt.% MMM at 35 ºC. Notice that in all these experiments the total pressure at the retentate side was kept at 330 kPa, the permeate side was kept at 125 kPa, and different CO_2/CH_4 mixtures (90/10, 50/50, 10/90 corresponding to CO_2 partial pressures of 297, 165 and 33 kPa, respectively) and single gas measurements (corresponding to CO_2 partial pressure of 330 kPa) were performed. Selectivity at 100 mol.% CO_2 corresponded to ideal selectivity and was calculated as the ratio of single gas permeabilities. For 16 wt.% MMM, the CO_2 permeate flow (cm^3 STP/min) linearly increases with the CO_2 partial pressure in the feed, i. e., with the amount of CO_2 molecules introduced in the system, as expected. In comparison with the ideal value, the selectivity slightly increased when CO_2/CH_4 mixed gases were tested. The highest value was obtained with 50/50 and 90/10 CO_2/CH_4 mixtures. This suggests that there was an apparent competitive adsorption of the gases, where at high

compositions of CO_2 the permeability of CH_4 decreases as a consequence of the faster diffusion of the smaller and more strongly adsorbed CO_2 gas molecule. For pure PSF, the highest selectivity value was reached for the 10/90 CO_2/CH_4 mixture, decreasing with the percentage of CO_2 in the feed composition. This may be due to the reduction of CO_2 solubility within the membrane since the adsorption sites become saturated, as occurred in other studies when the CO_2 pressure was increased [~~44~~45].

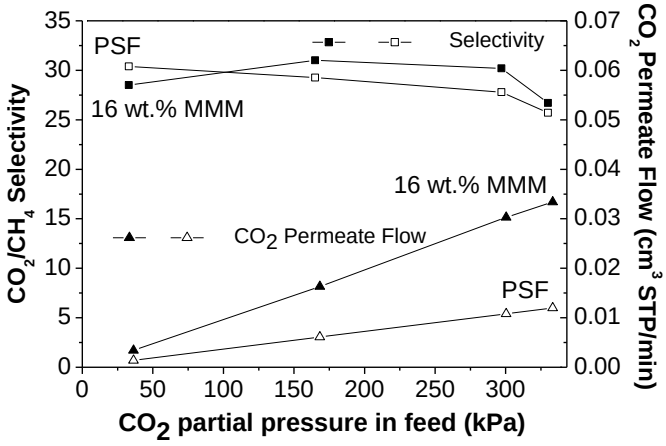

Fig. ~~10~~8. Effect of CO_2 partial pressure on selectivity and CO_2 permeate flow for CO_2/CH_4 mixtures at 35 ^oC and total pressure 330 kPa. Pure PSF (open symbols) and 16 wt.% MMM (closed symbols)

4. CONCLUSIONS

A new filler that combines micro- and meso-porosity has been used to prepare MMMs with polysulfone as the matrix, taking advantage of its spherical morphology and the hydrophobic character of the MOF ZIF-8 shell. This MOF shell made the silica core more compatible with the polymer, and in consequence these MMMs showed a good affinity between the polymer and the filler, which were well-dispersed throughout the thickness of the membrane. The preservation of the filler structure in the matrix was observed by XRD.

MSS-Z8 MMMs were tested for CO_2/CH_4 and H_2/CO_2 mixed-gas separations. In all the mixtures, the permeability increased with the filler content, while the selectivity remained almost constant with just a slight increase. Loadings of 32 wt.% MSS-Z8 provided the best improvement in terms of permselectivity, with an increase in permeability of almost 400 % for H_2 and 300 % for CO_2 in comparison with pure PSF. This permeability increase was attributed to the mesoporous phase of the silica core with bimodal pore distribution (2.7 and 10 nm), which may favor gas diffusivity, in addition to an enhancement of CO_2 adsorption with the incorporation of the filler in the case of CO_2 transport. Furthermore, no rigidification of the polymer was observed by DSC, indicating good filler-polymer compatibility. There was no loss of selectivity at high MSS-Z8 loadings with high levels of permeability, due to the good contact between filler and polymer, as well as the 3.4 Å pore of the ZIF-8 shell which acts as a molecular sieve.

In pure polymer and MSS-Z8 MMMs, the increase in temperature produced an improvement in permeability due to an increase in diffusivity of the gas as well as an enhancement in the motion and flexibility of the polymer chains. Selectivity decreased with the temperature for the CO_2/CH_4 mixture, while it increased for the H_2/CO_2 mixture.

For the H_2/CO_2 mixture, Robeson´s 2008 upper bound was reached by combining two factors: (a) the incorporation of 32 wt.% MSS-Z8 filler, and (b) the increase in temperature until 120 ºC. Finally, the effect of the feed composition for CO_2/CH_4 mixtures in 16 wt.% MMMs was studied, observing that the selectivity slightly increased when CO_2/CH_4 mixed-gases were tested, suggesting an apparent competitive adsorption of the gases.

ACKNOWLEDGEMENTS

Financial support from the Spanish Ministry of Economy and Competitiveness (MINECO, MAT2010-15870), as well as from the Regional Government of Aragón (DGA) and the European Social Fund (ESF), is gratefully acknowledged. S.S. acknowledges a grant from the DGA.

REFERENCES

[1] L. L. Cui, W. L. Qiu, D. R. Paul, W. J. Koros, Responses of 6FDA-based polyimide thin membranes to CO_2 exposure and physical aging as monitored by gas permeability, Polymer 52 (2011) 5528-5537.

[2] S. Basu, A. Cano-Odena, I. F. J. Vankelecom, MOF-containing mixed-matrix membranes for CO_2/CH_4 and CO_2/N_2 binary gas mixture separations, Sep. Purification Technol. 81 (2011) 31-40.

[3] A. L. Lee, H. L. Feldkirchner, S. A. Stern, A. Y. Houde, J. P. Gamez, H. S. Meyer, Field-tests of membrane modules for the separation of carbon-dioxide from low-quality natural gas, Gas Sep. Purif. 9 (1995) 35-43.

[4] A. L. Khan, A. Cano-Odena, B. Gutierrez, C. Minguillon, I. F. J. Vankelecom, Hydrogen separation and purification using polysulfone acrylate-zeolite mixed matrix membranes, J. Membr. Sci. 350 (2010) 340-346.

[5] D. Iarikov, S. Ted Oyama, Review of CO_2/CH_4 Separation Membranes, in: S. Ted Oyama, S. M. Stagg-Williams (Eds.), Inorganic, polymeric and composite membranes, Elsevier (2011), 91-115.

[6] M. K. Mondal, H. K. Balsora, P. Varshney, Progress and trends in CO_2 capture/separation technologies: A review, Energy 46 (2012) 431-441.

[7] M. G. Buonomenna, W. Yave, G. Golemme, Some approaches for high performance polymer based membranes for gas separation: block copolymers, carbon molecular sieves and mixed matrix membranes, RSC Adv. 2 (2012) 10745-10773.

[8] S. Basu, A. L. Khan, A. Cano-Odena, C. Liu, I. F. J. Vankelecom, Membrane-based technologies for biogas separations, Chem. Soc. Rev. 39 (2010) 750-768.

[9] L. M. Robeson, Correlation of separation factor versus permeability for polymeric membranes, J. Membr. Sci. 62 (1991) 165-185.

[10] L. M. Robeson, The upper bound revisited, J. Membr. Sci. 320 (2008) 390-400.

[11] S. Kulprathipanja, R. W. Neuzil, N. N. Li, Gas separation by means of mixed matrix membranes, Allied-Signal Inc., U.S. Patent, 4, 740, 219, (1988).

[12] T. S. Chung, L. Y. Jiang, Y. Li, S. Kulprathipanja, Mixed matrix membranes (MMMs) comprising organic polymers with dispersed inorganic fillers for gas separation, Prog. Polym. Sci. 32 (2007) 483-507.

[13] A. Brunetti, F. Scura, G. Barbieri, E. Drioli, Membrane technologies for CO_2 separation, J. Membr. Sci. 359 (2010) 115-125.

[14] B. Zornoza, C. Tellez, J. Coronas, Mixed matrix membranes comprising glassy polymers and dispersed mesoporous silica spheres for gas separation, J. Membr. Sci. 368 (2011) 100-109.

[15] S. Kim, E. Marand, High permeability nano-composite membranes based on mesoporous MCM-41 nanoparticles in a polysulfone matrix, Microporous Mesoporous Mater. 114 (2008) 129-136.

[16] O. M. Yaghi, M. O'Keeffe, N. W. Ockwig, H. K. Chae, M. Eddaoudi, J. Kim, Reticular synthesis and the design of new materials, Nature 423 (2003) 705-714.

[17] B. Zornoza, C. Tellez, J. Coronas, J. Gascon, F. Kapteijn, Metal organic framework based mixed matrix membranes: An increasingly important field of research with a large application potential, Microporous Mesoporous Mater. 166 (2013) 67-78.

[18] H. B. T. Jeazet, C. Staudt, C. Janiak, Metal-organic frameworks in mixed-matrix membranes for gas separation, Dalton Trans. 41 (2012) 14003-14027.

[19] R. Banerjee, H. Furukawa, D. Britt, C. Knobler, M. O'Keeffe, O. M. Yaghi, Control of pore size and functionality in isoreticular zeolitic imidazolate frameworks and their carbon dioxide selective capture properties, J. Am. Chem. Soc. 131 (2009) 3875-3877.

[20] K. S. Park, Z. Ni, A. P. Cote, J. Y. Choi, R. D. Huang, F. J. Uribe-Romo, H. K. Chae, M. O'Keeffe, O. M. Yaghi, Exceptional chemical and thermal stability of zeolitic imidazolate frameworks, Proc. Natl. Acad. Sci. U. S. A. 103 (2006) 10186-10191.

[21] S. Basu, M. Maes, A. Cano-Odena, L. Alaerts, D. E. De Vos, I. F. J. Vankelecom, Solvent resistant nanofiltration (SRNF) membranes based on metal-organic frameworks, J. Membr. Sci. 344 (2009) 190-198.

[22] M. J. C. Ordoñez, K. J. Balkus, J. P. Ferraris, I. H. Musselman, Molecular sieving realized with ZIF-8/Matrimid® mixed-matrix membranes, J. Membr. Sci. 361 (2010) 28-37.

[23] J. A. Thompson, K. W. Chapman, W. J. Koros, C. W. Jones, S. Nair, Sonication-induced Ostwald ripening of ZIF-8 nanoparticles and formation of ZIF-8/polymer composite membranes, Microporous Mesoporous Mater. 158 (2012) 292-299.

[24] Q. L. Song, S. K. Nataraj, M. V. Roussenova, J. C. Tan, D. J. Hughes, W. Li, P. Bourgoin, M. A. Alam, A. K. Cheetham, S. A. Al-Muhtaseb, E. Sivaniah, Zeolitic imidazolate framework (ZIF-8) based polymer nanocomposite membranes for gas separation, Energy Environ. Sci. 5 (2012) 8359-8369.

[25] Y. Dai, J. R. Johnson, O. Karvan, D. S. Sholl, W. J. Koros, Ultem®/ZIF-8 mixed matrix hollow fiber membranes for CO_2/N_2 separations, J. Membr. Sci. 401 (2012) 76-82.

[26] C. Zhang, Y. Dai, J. R. Johnson, O. Karvan, W. J. Koros, High performance ZIF-8/6FDA-DAM mixed matrix membrane for propylene/propane separations, J. Membr. Sci. 389 (2011) 34-42.

[27] M. Askari, T.-S. Chung, Natural gas purification and olefin/paraffin separation using thermal cross-linkable co-polyimide/ZIF-8 mixed matrix membranes, J. Membr. Sci. 444 (2013) 173-183.

[28] R. P. Lively, M. E. Dose, L. R. Xu, J. T. Vaughn, J. R. Johnson, J. A. Thompson, K. Zhang, M. E. Lydon, J. S. Lee, L. Liu, Z. S. Hu, O. Karvan, M. J. Realff, W. J. Koros, A high-flux polyimide hollow fiber membrane to minimize footprint and energy penalty for CO_2 recovery from flue gas, J. Membr. Sci. 423 (2012) 302-313.

[29] S. N. Wijenayake, N. P. Panapitiya, S. H. Versteeg, C. N. Nguyen, S. Goel, K. J. Balkus, Jr., I. H. Musselman, J. P. Ferraris, Surface cross-Linking of ZIF-8/polyimide mixed matrix membranes (MMMs) for gas separation, Ind. Eng. Chem. Res. 52 (2013) 6991-7001.

[30] K. Diaz, M. Lopez-Gonzalez, L. F. del Castillo, E. Riande, Effect of zeolitic imidazolate frameworks on the gas transport performance of ZIF8-poly(1,4-phenylene ether-ether-sulfone) hybrid membranes, J. Membr. Sci. 383 (2011) 206-213.

[31] A. F. Bushell, M. P. Attfield, C. R. Mason, P. M. Budd, Y. Yampolskii, L. Starannikova, A. Rebrov, F. Bazzarelli, P. Bernardo, J. C. Jansen, M. Lanc, K. Friess, V. Shantarovich, V. Gustov, V. Isaeva, Gas permeation parameters of mixed matrix membranes based on the polymer of intrinsic microporosity PIM-1 and the zeolitic imidazolate framework ZIF-8, J. Membr. Sci. 427 (2013) 48-62.

[32] B. Zornoza, B. Seoane, J. M. Zamaro, C. Téllez, J. Coronas, Combination of MOFs and zeolites for mixed-matrix membranes, Chem. Phys. Chem. 12 (2011) 2781-2785.

[33] K. Díaz, L. Garrido, M. López-González, L. F. d. Castillo, E. Riande, CO_2 transport in polysulfone membranes containing zeolitic imidazolate frameworks as determined by permeation and PFG NMR techniques, Macromolecules 43 (2010) 316-325.

[34] T. Yang, T.-S. Chung, High performance ZIF-8/PBI nano-composite membranes for high temperature hydrogen separation consisting of carbon monoxide and water vapor, Int. J. Hydrogen Energy 38 (2013) 229-239.

[35] T. Yang, G. M. Shi, T.-S. Chung, Symmetric and asymmetric zeolitic imidazolate frameworks (ZIFs)/polybenzimidazole (PBI) nanocomposite membranes for hydrogen purification at high temperatures, Adv. Energy Mater. 2 (2012) 1358-1367.

[36] S. Sorribas, B. Zornoza, C. Tellez, J. Coronas, Ordered mesoporous silica-(ZIF-8) core-shell spheres, Chem. Commun. 48 (2012) 9388-9390.

[37] B. Zornoza, S. Irusta, C. Tellez, J. Coronas, Mesoporous silica sphere-polysulfone mixed matrix membranes for gas separation, Langmuir 25 (2009) 5903-5909.

[38] B. Zornoza, O. Esekhile, W. J. Koros, C. Tellez, J. Coronas, Hollow silicalite-1 sphere-polymer mixed matrix membranes for gas separation, Sep. Purification Technol. 77 (2011) 137-145.

[39] N. Navascues, C. Tellez, J. Coronas, Synthesis and adsorption properties of hollow silicalite-1 spheres, Microporous Mesoporous Mater. 112 (2008) 561-572.

[40] Y. C. Pan, Y. Y. Liu, G. F. Zeng, L. Zhao, Z. P. Lai, Rapid synthesis of zeolitic imidazolate framework-8 (ZIF-8) nanocrystals in an aqueous system, Chem. Commun. 47 (2011) 2071-2073.

~~[41] P. Gorgojo, S. Uriel, C. Téllez, J. Coronas, Development of mixed matrix membranes based on zeolite Nu-6(2) for gas separation, Microporous Mesoporous Mater. 115 (2008) 85-92.~~

[~~42~~41] G. M. Shi, T. Yang, T. S. Chung, Polybenzimidazole (PBI)/zeolitic imidazolate frameworks (ZIF-8) mixed matrix membranes for pervaporation dehydration of alcohols, J. Membr. Sci. 415 (2012) 577-586.

[~~43~~42] T. Rodenas, M. van Dalen, E. García-Pérez, P. Serra-Crespo, B. Zornoza, F. Kapteijn, J. Gascon, Visualizing MOF mixed matrix membranes at the nanoscale: Towards structure-performance relationships in CO_2/CH_4 separation over NH_2-MIL-53(Al)@PI, Adv. Funct. Mater. (2013), DOI: 10.1002/adfm.201203462.

[~~44~~43] N. Liedana, A. Galve, C. Rubio, C. Tellez, J. Coronas, CAF@ZIF-8: One-Step Encapsulation of Caffeine in MOF, ACS Appl. Mater. Interfaces 4 (2012) 5016-5021.

[~~45~~44] W. Zhou, H. Wu, T. J. Udovic, J. J. Rush, T. Yildirim, Quasi-free methyl rotation in zeolitic imidazolate framework-8, J. Phys. Chem. A 112 (2008) 12602-12606.

[~~46~~45] C. A. Scholes, G. Q. Chen, G. W. Stevens, S. E. Kentish, Plasticization of ultra-thin polysulfone membranes by carbon dioxide, J. Membr. Sci. 346 (2010) 208-214.

[46] T.-H. Bae, J. S. Lee, W. Qiu, W. J. Koros, C. W. Jones, S. Nair, A high-performance gas-separation membrane containing submicrometer-sized Metal-Organic Framework crystals, Angew. Chem. Int. Ed. 49 (2010) 9863-9866.

[47] C. E. Powell, G. G. Qiao, Polymeric CO_2/N_2 gas separation membranes for the capture of carbon dioxide from power plant flue gases, J. Membr. Sci. 279 (2006) 1-49.

[48] H. Ettouney, U. Majeed, Permeability functions for pure and mixture gases in silicone rubber and polysulfone membranes: Dependence on pressure and composition, J. Membr. Sci. 135 (1997) 251-261.

Table 1. TGA loading and Tg of the different MMMs. These measurements are the average of three different samples.

Nominal loading (wt.%)	**TGA loading (wt. %)**	**Tg (ºC)**
0	0	188.5
8	7.7±0.6	190.2±0.6
12	11.6±1.1	188.8±0.7
16	16.1±0.7	189.9±0.0
20	20.3±0.8	189.7±0.5
32	29.7±0.6	189.8±0.2

Table 2. Apparent activation energies of CO_2, CH_4 and H_2 calculated from equimolar CO_2/CH_4 and H_2/CO_2 mixtures for pure PSF and 16 and 32 wt.% MMMs.

	E_p (kJ/mol)			
	CO_2	**CH_4**	**H_2**	**CO_2**
PSF	12.1	27.8	17.9	9.6
16 wt.% MMM	11.0	25.7	-	-
32 wt.% MMM	10.4	24.7	16.4	10.2